Proc. Natl. Acad. Sci. USA
Vol. 95, pp. 6175–6180, May 1998
Cell Biology

Transcytosis of α_1-acidic glycoprotein in the continuous microvascular endothelium

D. PREDESCU, S. PREDESCU, T. MCQUISTAN, AND G. E. PALADE*

Division of Cellular and Molecular Medicine, University of California at San Diego, School of Medicine, La Jolla, CA 92093

Contributed by George E. Palade, March 13, 1998

ABSTRACT **By using perfusions and bolus administration, coupled with postembedding immunocytochemical procedures, we have identified the structures involved in the transport of derivatized orosomucoid (α_1-acidic glycoprotein) across the continuous microvascular endothelium of the murine myocardium. Our findings indicate that: (*i*) monomeric orosomucoid binds to the luminal surface of the endothelium; (*ii*) it is restricted to caveolae during its transport across the endothelium; (*iii*) it is detected in the perivascular spaces at early time points (by 1 min) and in larger quantities at later time points (>5 min) from the beginning of its perfusion or its intravascular administration; (*iv*) no orosomucoid molecules are found in the intercellular junctions or at the abluminal exits of interendothelial spaces; and (*v*) the vesicular transport of orosomucoid is strongly inhibited by *N*-ethylmaleimide (>80%). Because, by size and shape, the orosomucoid qualifies as a preferential probe for the postulated small pore system, our results are discussed in relation to the pore theory of capillary permeability.**

α_1-Acidic glycoprotein [referred throughout this paper as orosomucoid (Om)] is a glycoprotein of 41,000 Da that measures $\approx 30 \times 30 \times 60$ Å (1) and is normally found in the blood plasma at a concentration of 0.7–1.0 g/liter (2). It is produced in the liver and its clearance also appears to occur predominantly in the liver, although some renal excretion is possible, particularly at high Om concentrations (3). Available data indicate that Om, together with albumin and other plasma proteins (4, 5), modifies the permeability of the vascular endothelium, presumably by interacting with the endothelial glycocalyx to form an additional permselective barrier referred in the literature as the fiber matrix (6). Because Om has a pI around 2.7–3.0, it has been suggested that its binding to the glycocalyx increases the negative charge of the luminal surface of the vessel wall (7).

Om is also found in the lymph as a normal constituent, but the lymph/plasma ratio varies from one microvascular bed to another without an obvious correlation with the local type of endothelium. Distribution studies performed with ^{125}I-labeled Om (^{125}I-Om) have shown that $\approx$40% of the amount administered *in vivo* distributes throughout the body in the extravascular compartment (8).

We have designed and applied a protocol (9, 10) that uses derivatized proteins as tracers that can be individually and directly detected by electron microscopy (EM) immunocytochemistry under conditions of satisfactory endothelial preservation. This protocol also allows the quantitation of tracer transported to the interstitial fluid.

The results obtained in our experiments indicate that: (*i*) in different murine microvascular beds, provided with a continuous endothelium (heart, diaphragm) Om binds to the luminal surface of the endothelium; (*ii*) it is transported across the endothelium exclusively by caveolae; (*iii*) its endothelial transcytosis is *N*-ethylmaleimide (NEM)-sensitive; and (*iv*) the binding, and probably the transport, of Om involves three different proteins with M_r below 25,000.

MATERIALS AND METHODS

Animals. Male BALB/c mice (20–25 g) were kept under standard housing and feeding conditions, and all the experiments were done while the animals were under anesthesia obtained by intraperitoneal administration of a mixture of ketamine and xylazine (0.1 ml/100 g of body weight).

Materials. Reagents and supplies were obtained as indicated below: PBS (with Ca^{2+} and Mg^{2+}), medium 199, fetal calf serum (FCS), and Hepes from GIBCO; phenylmethanesulfonyl fluoride (PMSF), Om, 3-[(3-cholamidopropyl)dimethylammonio]-1-propanesulfonate (CHAPS), NEM, poly(L-glutamic acid) (M_r 18,000), BSA (fraction V), and potassium carbonate from Sigma; 3,3′,5,5′-tetramethylbenzidine (TMB) from Kirkegaard & Perry Laboratories; P-10 desalting columns, Sephadex G-100, Pharmalyte ampholytes, and agarose (isoelectric focusing grade) from Pharmacia Biotech; paraformaldehyde, glutaraldehyde, glutamic acid, and tetrachloroauric acid from Electron Microscopy Sciences (Fort Washington, PA); rabbit anti-dinitrophenyl (DNP) IgG, horseradish peroxidase-conjugated anti-DNP IgG, and affinity-purified goat anti-rabbit IgG from Dako; dinitrobenzenesulfonic acid (DNBS) from Aldrich; Na^{125}I (carrier free) and sheep red blood cells from ICN Pharmaceuticals; ketamine hydrochloride and xylazine at 100 mg/ml active substance from Aveco (Fort Dodge, IA); Bolton–Hunter reagent and ^{51}Cr from Amersham; human umbilical vein endothelial cells from Clonetics (San Diego); and bovine endothelial cells (from pulmonary artery, pulmonary vein, and lung microvasculature) from the American Type Culture Collection (Manassas, VA).

Type of Tracers. We have used both monomeric derivatized Om (as a preferential probe for the postulated small pore system) and colloidal gold–Om complexes (as an exclusive probe for the postulated large pore system) to visualize their interactions with the endothelial cells and to identify the pathways and mechanisms of their efflux. Om adsorbed on 22-nm colloidal gold particle (Om–Au) was used only for perfusions, whereas derivatized Om (Om-DNP), detected by postembedding immunocytochemistry, was employed in perfusions and bolus administrations. Om-DNP was used to quantitate the amount of tracer transported and to find out whether NEM has any effect on its endothelial transport. Control experiments with ^{125}I-Om and ^{125}I-Om-DNP were

Abbreviations: Om, orosomucoid (α_1-acidic glycoprotein); EM, electron microscopy; NEM, *N*-ethylmaleimide; DNP, dinitrophenyl; TMB, 3,3′,5,5′-tetramethylbenzidine; CHAPS, 3-[(3-cholamidopropyl)dimethylammonio]-1-propanesulfonate.

*To whom reprint requests should be addressed at: Division of Cellular and Molecular Medicine, University of California at San Diego, School of Medicine, 9500 Gilman Drive, La Jolla, CA, 92093-0602. e-mail: gpalade@ucsd.edu.

The publication costs of this article were defrayed in part by page charge payment. This article must therefore be hereby marked "*advertisement*" in accordance with 18 U.S.C. §1734 solely to indicate this fact.

used to check the possibility that derivatization of Om may affect means and routes of Om transport.

Perfusion Experiments. The protocol used was the same as in ref. 11. Briefly, the abdomen was opened, a cannula placed ≈1 cm cranial to the iliac bifurcation in the abdominal aorta was used as the inlet, and an opening made in the vena cava caudalis provided the outlet. The vasculature was perfused by using a peristaltic pump (type P1 Pharmacia) at a flow rate of 3 ml/min with PBS supplemented with 2 g/liter glucose and oxygenated by passing it through a mixture of 95% O_2 and 5% CO_2 (supplemented PBS or sPBS). The hydrostatic pressure, under these conditions, is assumed to be close to the normal blood pressure (12). In the experiments in which the NEM effect was tested, the vascular bed was perfused for 5 min before the tracer with 1 mM NEM in sPBS, followed by 15 min perfusion with the tracer solution containing the same NEM concentration. At the end of each perfusion, the vasculature was flushed free of tracer by perfusing it for 5 min with sPBS. This step was promptly followed by (*i*) removal of the hearts used in biochemical assays or (*ii*) fixation by perfusing the vasculature for 10 min with a mixture of 3% formaldehyde (freshly prepared from paraformaldehyde) and 2.5% glutaraldehyde made in 0.1 M sodium cacodylate buffer, pH 7.2, for tissue specimens to be processed for EM and immunocytochemistry.

Bolus Administration. The protocols used for bolus administration of the tracers were as in ref. 13. At different time points after Om-DNP administration (0.2 ml from a solution of 50 mg/ml), the same fixative mixture as in perfusion experiments was injected intraperitoneally and intrapleurally and after ≈10 min of *in situ* fixation, myocardium and diaphragm samples were removed, cut in small pieces (≈2 × 2 mm) and processed as described for the standard EM procedure (see below). Bolus administrations of radiolabeled Om were done by injecting 100 μl of a mixture of ^{125}I-Om or ^{125}I-Om-DNP and ^{51}C-labeled sheep red blood cells, into a tail vein.

Preparation of Tracers. Colloidal gold particles with an average diameter of 22 nm were obtained by citrate reduction of a tetrachloroauric acid solution (14). The particles were stabilized with Om (30 μg/ml) and diluted to A_{520} = 1. Reporter antibody conjugates were prepared by adsorbing on 5- or 8-nm colloidal gold particles (obtained by tannic acid/sodium citrate reduction) an affinity-purified goat anti-rabbit IgG at a concentration of 50 μg/ml (15). Secondary stabilization of the gold suspensions was obtained by poly(L-glutamic acid) (200 μg/ml) as in ref. 16. Just before use, the concentrated IgG-Au stock solutions were diluted in PBS to give A_{520} = 0.2–0.3 and centrifuged for 1 h at 40,000 × *g* to remove gold aggregates. Bovine Om was tagged with DNP as in ref. 17. Briefly, 250 mg of Om dissolved in 15 ml of water containing 250 mg of potassium carbonate was reacted with 250 mg of dinitrobenzenesulfonic acid for 20 min at room temperature. The mixture was passed first over a P-10 desalting column and then over a Sephadex G-100 column (1 cm × 90 cm) to obtain monomeric Om-DNP free of DNBS. The Om-DNP was characterized by nondenaturing SDS/PAGE and by isoelectric focusing in 1% agarose. The average number of DNP residues per Om molecule was estimated, by using a molar extinction coefficient of 17,530 for DNP-lysyl and a molecular weight of 41,000 for Om, as in ref. 17.

Bovine Om and bovine Om-DNP were radioiodinated to a specific radioactivity of ≈2 μCi/mg (1 μCi = 37 kBq) by using the Bolton–Hunter reagent (18). Sheep red blood cells were labeled with ^{51}Cr (19).

EM and Immunocytochemistry. The tissues were perfused with Om-Au for selected times and then fixed for 10 min by perfusion as described under *Perfusion Experiments*. Collected specimens were further fixed by immersion in a triple fixative (20) for 60 min on ice, then stained in block for 30 min in 7.5% uranyl magnesium acetate, dehydrated slowly in graded ethanol solutions, and embedded in Epon. This was the standard procedure for EM in all experiments.

Om-DNP was detected by a postembedding immunostaining procedure. After the free tracer had been removed by flushing the vasculature for 3–5 min with sPBS, specimens were fixed as described above and processed for embedding and microtomy. Sections of ≈50–60 nm, quenched for 30 min in PBS + 1% BSA (A-PBS), were incubated first for 1–2 h in anti-DNP IgG diluted 1:2000 in A-PBS and then for 1 h with gold-tagged goat anti-rabbit IgG diluted 1:5000 in A-PBS. All sections were examined and micrographed in a Philips CM 10 electron microscope.

Cell Culture and Cell Lysates. Each type of endothelium was grown to confluence in two 150-cm^2 surface plastic Petri dishes and used 3 days later. The confluent layers were washed three times for 1 min each with cold PBS, then removed with a cell scraper, resuspended in 2 ml of PBS, and sedimented at maximum speed in a Fisher model 235B microcentrifuge for 30 sec. The pellet was solubilized in a lysis buffer (20 mM CHAPS, 1 mM phenylmethanesulfonyl fluoride in PBS, pH 7.2), by gently shaking it for 1 h at room temperature. The cell lysate was cleared by centrifugation for 1 h at 40,000 rpm in a Beckman TL-100 ultracentrifuge using the TLA-45 rotor.

Tracer Transport and Its NEM Inhibition. The heart vasculature, perfused as described, was flushed free of tracer by perfusing it with sPBS for 5 min. The hearts were removed and the ventricles were weighed, hand minced, and homogenized in a Polytron (Brinkmann) at 1:10 (wt/vol) ratio in PBS. The ensuing homogenate was centrifuged at 150,000 × *g* in a Beckman table-top ultracentrifuge for 1 h at 4°C, using a TLA 45 rotor. The pellet was discarded and the final supernatant, expected to include the interstitial fluid of the myocardium, was assayed for its total protein and Om-DNP content. Om-DNP transported in 15 min to the interstitial fluid was determined in the final supernatant by ELISA using Om-DNP as a standard, a horseradish peroxidase-tagged anti-DNP antibody as reporter, and TMB as peroxidase substrate. The readings were done at 650 nm in a Molecular Dynamics ELISA reader. The same general protocol was used to assess NEM effects in experiments in which this reagent was included.

Protein Determination. Protein content was determined by the micro bicinchoninic acid assay (21) with BSA as standard.

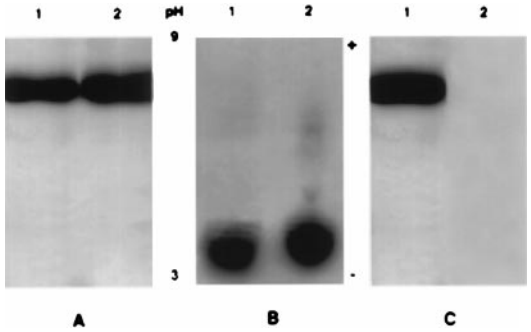

FIG. 1. Characterization of the tracers. (*A*) The derivatized Om as well as the native molecule have the same migration behavior in SDS/PAGE. Om-DNP (5 μg) in lane 1 and native Om (5 μg) in lane 2 were run at 150 V for 90 min. The minigels were stained with Coomassie blue R-250. (*B*) Immunoelectrophoresis on a 1% agarose gel shows that the net electric charge of Om-DNP (lane 1) is not significantly different from that of native Om (lane 2). The ampholytes used were pH 3–9, and the direction of pH gradient is indicated by the + and − signs. Every lane was loaded with 7 μg of protein. (*C*) SDS/PAGE of Om-DNP transferred to nitrocellulose paper (1 h at 700 mA) and blotted with anti-DNP antibody (diluted 1:2000). Only Om-DNP is recognized by the antibody (lane 1); the native Om in lane 2 does not give a signal. Each lane was loaded with 5 μg of protein.

Ligand Blotting. Nondenaturing SDS/PAGE was performed as in ref. 22 with a preparative SDS/5–20% polyacrylamide minigel. The electrophoretograms were transferred (2 h, at 700 mA and 4°C) to nitrocellulose membranes. The transfers were stained with 2% Ponceau S, dried, and stored. The nitrocellulose was cut in ≈3-mm-wide strips, blocked overnight with 5% BSA + 0.05% Tween 20 in PBS (AT-PBS), then incubated for 2 h with ^{125}I-Om diluted to a specific activity of 0.4 μCi/ml in AT-PBS. After extensive washing with AT-PBS, the strips were exposed to a Kodak XAR 5 film and developed with a Kodak X-Omat processor.

RESULTS

Om-DNP Properties. SDS/PAGE and isoelectric focusing used to characterize Om-DNP showed that the derivatization process did not significantly affect the molecular weight (Fig. 1*A*) and the overall electric charge of Om (Fig. 1*B*). Fig. 1*C* shows that the anti-DNP antibody recognizes only Om-DNP and not the native Om. On these accounts, Om-DNP appears to be a close enough approximation of native Om to justify its use as an experimental substitute for the latter. We calculated that 4 to 6 lysine residues, out of 12, were derivatized and could be available for immunodetection on the surface of thin sections of satisfactorily preserved specimens because the DNP epitope survives OsO_4 fixation and plastic embedding (10).

Om in Perfused Specimens. When the heart microvasculature was perfused for less than 5 min, we found the tracer bound to the endothelial surface and the bound Om-DNP could be removed by flushing the vasculature with sPBS (data not shown). By 5 min, however, the bound tracer could no longer be removed by flushing, and heavy Om-DNP labeling was found on the plasmalemma proper as well as on caveolae (Fig. 2 *A–C*). We assume that tracer binding begins and progresses as the native Om is removed by the perfusate from the surface of endothelial cells. There was no preferential association with structural elements of plasmalemma proper or intercellular junctions. We found, however, filtration residues as in ref. 11 on the introits (luminal side) of intercellular junctions (micrographs not shown). Past 2–3 min, the tracer was found within the endothelium restricted to caveolae apparently free in the cytoplasm or opened on the abluminal front (Fig. 2*A*). After 5 min it was found scattered in small numbers in the perivascular spaces (Fig. 2*B*), where its density increased with time (Fig. 2 *B* and *C*). Never did we find Om-DNP within intercellular junctions or associated preferentially with the abluminal exit of intercellular spaces. The

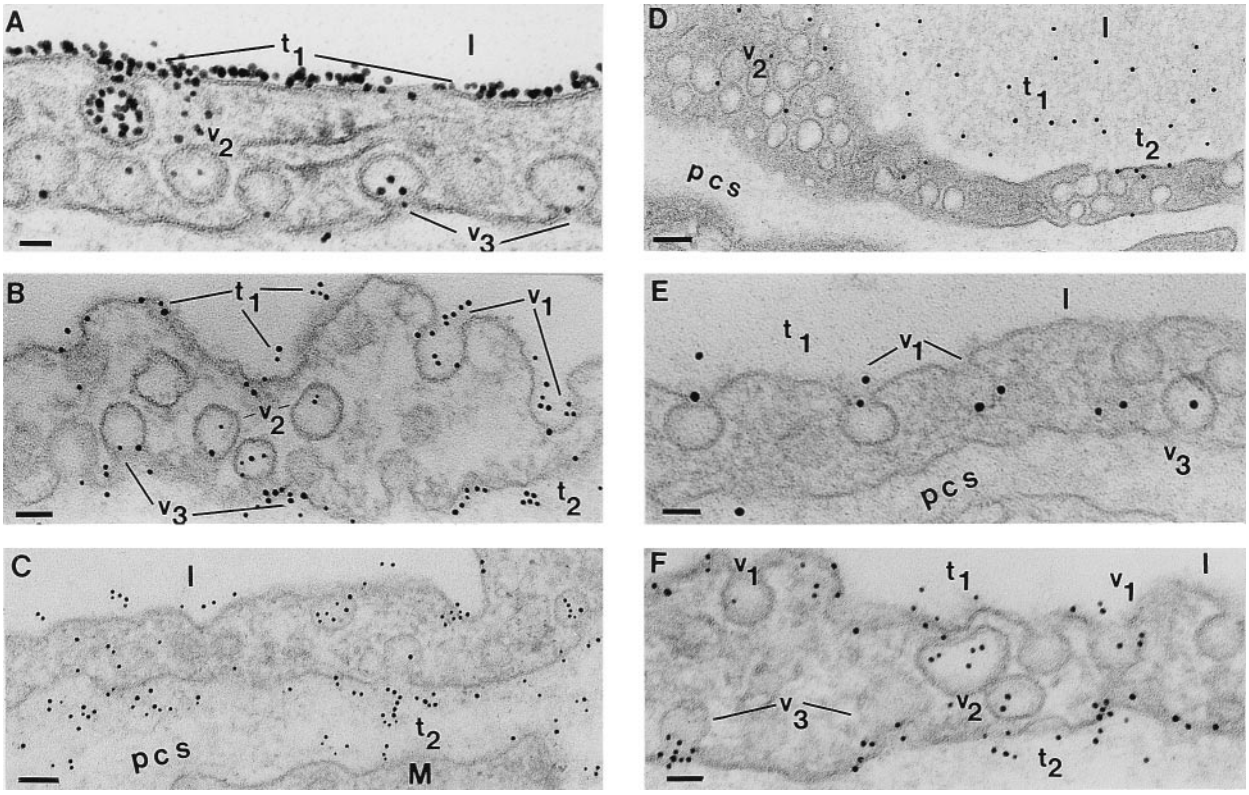

FIG. 2. Postembedding immunodetection of Om-DNP in perfused and bolus-administered specimens. (*A*) Capillary profile in a specimen perfused for 5 min with Om-DNP (at 5 mg/ml). The luminal endothelial surface is extensively labeled by the tracer (t_1). Inside the endothelium only a few caveolae (v_2) are labeled, but even at this early time, caveolae (v_3) discharging their content could be seen. l, lumen. (Bar = 35 nm.) (*B*) After 15 min Om-DNP molecules are associated with the luminal plasmalemma (t_1), with caveolae opened to the lumen (v_1), with caveolae apparently free in the cytosol (v_2), and with caveolae that are discharging their content into the pericapillary spaces (v_3). Note also the presence of apparently free tracer molecules (t_2) in the perivascular spaces. (Bar = 60 nm.) (*C*) As time of perfusion progresses (30 min), the tracer is found all over the endothelial profile with the same distribution as in *B,* but the label density (t_2) over the perivascular spaces is much more extensive. M, muscle; pcs, pericapillary space(s). (Bar = 84 nm.) (*D*) After 5 min of an i.v. injection of 100 μl from a concentrated Om-DNP solution (of 50 mg/ml), the tracer is present in the lumina of the vessels (t_1), associated with the plasmalemma proper (t_2), with the caveolae opened to the luminal and abluminal (v_3) side of the endothelium, and with caveolae apparently free in the cytosol (v_2). (Bar = 100 nm.) (*E*) At 15 min from bolus administration of Om-DNP the majority of the tracer is still found in the lumen (t_1). The tracer molecules label more extensively caveolae opened to the lumen (v_1) as well as caveolae that are discharging their content (v_3) in the perivascular spaces. (Bar = 52 nm.) (*F*) Thirty minutes after i.v. administration, the tracer is still found in the lumina (t_1) but many caveolae opened to the lumen (v_1) or scattered inside the cells (v_2) are labeled, as are the caveolae (v_3) discharging on the abluminal front of the cell; some of the latter contain multiple tracer molecules. Note the extensive labeling (t_2) of the perivascular spaces at this time, resembling that found in perfused specimens; yet its density remains much lower than that encountered in perfused specimens (compare with *C*). (Bar = 53 nm.)

same pattern of Om-DNP distribution was found in the microvasculature of heart and diaphragm.

When Om-Au (22 nm) was perfused, its binding to the endothelial surface, labeling of caveolae, and transport to the perivascular spaces were comparable, but less extensive, than in the case of Om-DNP. Interestingly, the large tracer was found plugging, single or in pairs, the neck of luminaly opened caveolae (Fig. 3*A*) and also the necks of caveolae opened abluminaly (Fig. 3*B*). The meaning of these unexpected findings will be explained in a subsequent paper.

Om in Bolus-Administered Specimens. Om-DNP was found uniformly distributed over the lumina of vascular profiles with no evidence of any lack of capillary recruitment throughout the examined tissues. The endothelial plasmalemma proper and the caveolae were the only labeled structures on the luminal aspect of the cells (Fig. 2 *D–F*), but the labeling was, strikingly, less extensive than in Om-DNP-perfused specimens (compare Fig. 2 *A* and *D*). This difference could be explained by the presence of endogenous Om bound to the endothelium in specimens obtained after bolus administration and its progressive and extensive removal from perfused specimens. Past 5 min, labeled caveolae acquired a uniform distribution across the endothelium (Fig. 2 *E* and *F*). The tracer was detected in the perivascular spaces after 5 min (Fig. 2 *E* and *F*) and its local concentration increased progressively with time, but even by 30 min (Fig. 2*F*) large differences in Om-DNP concentration between blood plasma and interstitial spaces remained evident. No tracer was found in the intercellular junctions and no concentration of Om-DNP in the perivascular spaces around the abluminal exit of the intercellular spaces was recorded at any time.

Quantitation of Om Transcytosis. We used the perfused mouse hearts to measure the amount of Om-DNP transported to the interstitial fluid and normalized it to total protein determined in the final supernatants of heart homogenates. Because the myocardial microvasculature was flushed free of Om-DNP at the end of perfusions, we assume that the majority of the tracer was in the interstitial fluid and we did not take into consideration the tracer scattered inside the vascular endothelium. We found an average of 279.2 ± 31.9 ng of Om-DNP per mg of wet tissue per 5 min transported to the interstitial fluid (50 animals used). This value is in agreement with data already published for other tracers qualified as preferential probes for the postulated small pore system (10).

Fig. 4 documents the effect of NEM on the transendothelial transport of Om-DNP. When the myocardial vasculature was perfused with 1 mM NEM for 5 min followed by Om-DNP in the presence of the same concentration of NEM for 15 min, we found an 80–85% inhibition of tracer transport (Fig. 4*A*), by reference to controls (no NEM). The results obtained by EM and immunocytochemistry on NEM-perfused specimens (Fig. 4*B*) showed that NEM does not affect the normal morphology of the murine heart microvasculature even after 20 min of exposure to 1 mM NEM. In the absence of any detectable change in either intercellular junctions or caveolar structure, we found reduced amounts of Om-DNP in the perivascular spaces (Fig. 4*B*).

To check the possibility that this tracer behaves differently from native Om, we performed control experiments in which

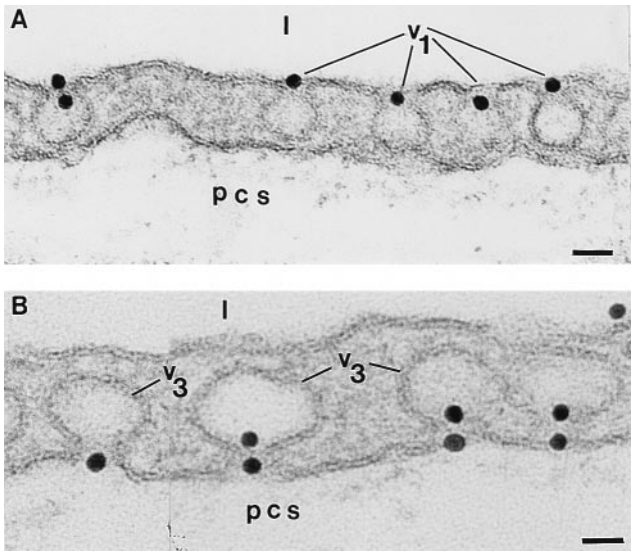

FIG. 3. Binding pattern of Om-Au. (*A*) When Om-Au (≈22 nm diameter) was perfused as in Fig. 2 *A–C*, the necks of many caveolae opened to the lumina (v_1) were plugged by the tracer. (Bar = 49 nm.) (*B*) By 15 min of perfusion, the gold coated particles are seen plugging the necks of the caveolae (v_3) opened on the abluminal front of the cells. Not so often, the necks of some caveolae (v_3) opened on the tissular side of endothelial cells are plugged with two gold particles. (Bar = 28 nm.) l, lumen; pcs, pericapillary space(s); the same abbreviations are used for Fig. 4.

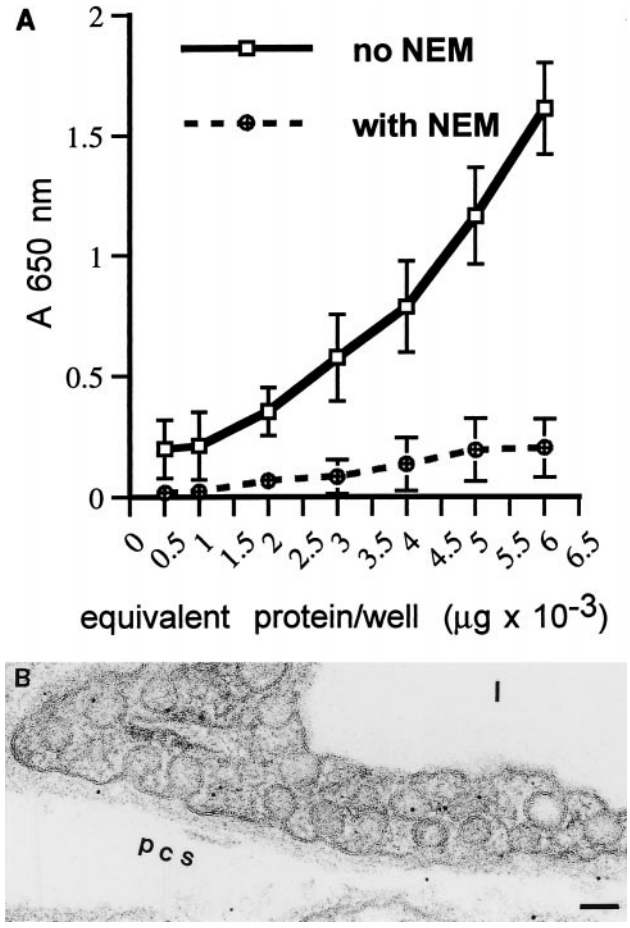

FIG. 4. NEM effect on Om-DNP transcytosis. (*A*) Graphic representation of the amount of Om-DNP, expressed as protein equivalents, transported in the presence of NEM (broken line) and in the absence of NEM (continuous line) in perfused murine hearts. Tracer amounts were determined in 8–10 consecutive experiments (4–6 mice per experiment), and ELISAs were performed in duplicates for three different dilutions. Tracer perfusions were for 15 min as described in the text. Every point on the graphs is a mean value of ≈35 determinations with standard deviation given. (*B*) An electron micrograph taken from one of the mice used to quantitate Om-DNP transcytosis in the presence of NEM. The normal endothelial morphology, the lack of any detectable structural alteration, and the drastic reduction in labeling of endothelial caveolae and perivascular spaces (compare with Fig. 2 *B*, *C*, *E*, and *F*) at the end of a 20-min exposure to 1 mM NEM are illustrated by this micrograph. (Bar = 84 nm.)

^{125}I-Om was administered as a bolus, instead of Om-DNP. To estimate the vascular and extravascular volumes of Om distribution, two lots of mice (each having 50 mice) were injected with 100 μl of ^{125}I-Om (6.8×10^8 cpm) + ^{51}Cr-labeled sheep red blood cells (4.06×10^5 cpm). At selected intervals blood samples were obtained and their ^{125}I and ^{51}Cr radioactivities were determined; then the hearts were excised and processed as in Om-DNP experiments to prepare a final supernatant in which the two types of radioactivity were assayed. From these data we calculated: (*i*) the vascular volume, (*ii*) the apparent distribution volume of labeled Om, and (*iii*) the amount of Om transported to the interstitial fluid of the myocardium. The vascular volume was estimated at 2.17 ml ± 0.22 (97 mice); the ^{125}I-Om extravascular distribution reached ≈40% of the initial administered activity by 20 min, and the amount of tracer transported to the interstitial fluid was calculated at 196.2 ± 16.8 ng of ^{125}I-Om per mg of wet tissue per 5 min (97 animals). These values are lower than the values obtained in perfusion experiments, but we consider that the endogenous Om acts as a competitor. Parallel experiments with ^{125}I-Om-DNP give the same results as ^{125}I-Om (data not shown), a fact that leads us to believe that derivatized Om is an acceptable approximation of the native molecule.

Detection of Om Binding Proteins. To better define the Om interactions with the endothelium, we have used total cell lysates from cultured human and bovine endothelial cells, resolved by SDS/PAGE, transferred to nitrocellulose membranes, and probed with ^{125}I-Om. These ligand overlays revealed, by autoradiography, a doublet in the 20- to 14-kDa range, a single band around 7 kDa, and in some endothelia a band of ≈10 kDa (Fig. 5). Om binding to these proteins was blocked by competition with native Om but not by albumin, hemoglobin, or IgG (data not shown). The same protein pattern was found when endothelial lysates from large vessels as well as from microvasculature were used.

DISCUSSION

In this project we have extended to Om an experimental protocol we worked out a few years ago (9, 10). The tracers used in ref. 10 as probes for the postulated small pore system are rather experimental than physiological. Om was selected as a tracer because it is a normal constituent of the blood plasma, interstitial fluid, and lymph and because, on account of its shape and molecular dimensions, it qualifies as a preferential probe for the small pore system postulated by the capillary physiologists.

EM immunocytochemical detection of Om-DNP on myocardium specimens from experiments done by perfusion or bolus administration has shown that the tracer binds to the luminal plasmalemma of the endothelium, gains access to caveolae to which it is strictly restricted while in transit across the endothelium, and appears in time (by 1 min) in the pericapillary spaces. The caveolae open to the luminal front contain many Om-DNP molecules, whereas the content of their counterparts open to the abluminal front varies from one to many.

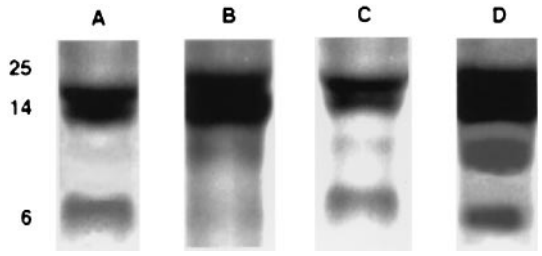

FIG. 5. Detection of Om binding proteins by ligand blotting. Lysates of different endothelial cell types—namely bovine microvascular cells (*A*), bovine pulmonary vein (*B*), bovine pulmonary artery (*C*), and human umbilical veins (*D*)—were subjected to electrophoresis on SDS/5–20% polyacrylamide minigels under nondenaturing conditions. After transfer, the nitrocellulose strips were incubated with ^{125}I-Om for 1 h at room temperature, washed extensively, and exposed to Kodak XAR 5 film for 1 h. Apparent molecular masses in kDa are indicated on the side. In all endothelial cell types so far examined, we found an upper doublet within 14–20 kDa and a third, lower, band around 7 kDa.

We found no evidence of Om-DNP exit through intercellular junctions, a finding that is not in agreement with the conclusions formulated by capillary physiologists who have postulated the presence of small pores along intercellular junctions.

The results of control experiments carried out with ^{125}I-Om (instead of Om-DNP) have shown that this tracer is transported efficiently to the interstitial fluid of the murine myocardium.

Because Om-DNP binds extensively to the surface of endothelium (Fig. 2*A*), we surveyed different endothelia and found that ^{125}I-Om binds to a similar group of proteins in bovine and human endothelia. Their role in microvascular permeability remains to be explored and defined. As already published (23), Om binds to specific, but not yet fully characterized, sites on the endothelial surface; hence the proteins detected in this study may be involved in this specific interaction.

Om-Au complexes of ≈22 nm diameter were prepared and used as exclusive probes for the postulated large pore system. Because they are coated with the same protein used as a small pore probe, we assume that any difference recorded between Om-Au and Om-DNP can be ascribed, primarily, to differences in size. In perfusion experiments with Om-Au, the probe bound to the luminal plasmalemma, gained access to some caveolae, remained restricted to caveolae within the endothelium, and appeared in time (by 2 min) in the perivascular spaces. Moreover, the probe was found plugging the introit of many caveolae open on the luminal as well as on the abluminal front of the endothelium (Fig. 3). As in the case of Om-DNP, we found no evidence of Om-Au exit through intercellular junctions. These findings imply that caveolae function as structural and functional equivalents of the postulated small pore system as already discussed in ref. 10 and in this paper, as well as equivalents of the postulated large pore system, a point documented here and in previous work from a number of laboratories (24–27). We assume that in the cycle of its function, each caveola acts as a large pore equivalent when fully opened and as a small pore equivalent when the opening is constricted to ≤10 nm. This hypothesis, which attempts to explain some of the basic tenets of the pore theory of capillary permeability in terms of our recent findings, is now under investigation in our laboratory.

Our experimental protocol comprised a biochemical moiety, complementary to the morphological and immunocytochemical moieties, all of them discussed above. The role of the morphological part was to identify the structures, to suggest the mechanisms involved in transendothelial exchanges, and to check at the end of each experiment the condition (intact or damaged) of the endothelium. The biochemical part made possible the quantitation of transport across the endothelium and, in addition, strengthened significantly the evidence for transcytosis by showing that NEM drastically inhibits (>80%) Om-DNP transport to a tissue fraction that includes the interstitial fluid of the myocardium. At the end of NEM perfusions, morphological controls revealed no detectable damage to the endothelium, but illustrated reduced Om-DNP transport to perivascular spaces (Fig. 4*B*). In previous reports, we (10) and others (28) have shown that the transport of small molecules such as sucrose (diameter ≈1 nm) and inulin [5.9×1.5 nm, but easily convertible into a thin (≈1 nm) thread] is not sensitive to NEM, presumably because such molecules follow

the paracellular pathway as in a leaky epithelium. NEM is known to inactivate NSF (NEM-sensitive Factor) the ATPase that is a key component of the membrane fusion machine involved in many types of vesicular transport (29, 30) including transcytosis. Recent findings indicate that NSF and other factors (SNAPs and v- and t-SNAREs) involved in targeting, fusion, and fission of vesicular carriers are present in cells of the continuous microvascular endothelium (9, 31).

As a cellular process in which a caveola recycles from one front to another of the endothelium, transcytosis is expected to be amenable to regulation by intra- and extracellular factors. In this report we have shown again that NEM drastically curtails the rate of transcytosis by inactivating NSF, a critical component of the membrane fusion machine (29). Fusion of a caveola with the target membrane requires a fusion machine, but its detachment, in preparation for another round trip, requires membrane fission, a process in which other factors, such as the 100-kDa GTPase dynamin, are implicated (32, 33). Dynamin is also present in endothelial cells (34). Notwithstanding the relative large volume of the earlier literature dealing with transcytosis in the continuous microvascular endothelium (24, 35, 36) many capillary physiologists have ignored it or denied its significance for blood/interstitial fluid exchanges (37). Only recently, some capillary physiologists (38) began taking into consideration the significance of transcytosis for blood/interstitial fluid exchanges. As the evidence in support of transcytosis becomes stronger, new questions arise for which answers must be provided in the future.

This study was supported by National Heart, Lung, and Blood Institute Grant HL-17080.

1. McPherson, A., Friedman, M. L. & Halsall, H. B. (1984) *Biochem. Biophys. Res. Commun.* **124,** 619–624.
2. Schmid, K. (1975) in *The Plasma Proteins*, ed. Putnam, F. W. (Academic, San Francisco), Vol. 1, pp. 183–229.
3. Schmid, K. (1989) in *Alpha$_1$-Acid Glycoprotein: Genetics, Biochemistry, Physiological Functions and Pharmacology*, eds. Baumann, P., Müller, W. E., Eap, C. B. & Tillement, J.-P. (Liss, New York), pp. 7–22.
4. Haraldsson, B. (1985) *Acta Physiol. Scand.* **123,** 427–436.
5. Haraldsson, B. & Ripe, B. (1987) *Acta Physiol. Scand.* **129,** 127–135.
6. Curry, E. E. & Michel, C. C. (1980) *Microvasc. Res.* **20,** 96–99.
7. Curry, F. E., Rutledge, J. E. & Lentz, J. F. (1989) *Am. J. Physiol.* **257,** H1354–H1359.
8. Gross, V., Heinrich, P. C., vanBerg, D., Steube, K., Tran-Thi, T. A., Decker, K. & Erok, W. G. (1989) in *Alpha$_1$-Acid Glycoprotein: Genetics, Biochemistry, Physiological Functions and Pharmacology*, eds. Baumann, P., Müller, W. E., Eap, C. B. & Tillement, J.-P. (Liss, New York), pp. 231–234.
9. Predescu, D., Horvat, R., Predescu, S. & Palade, G. E. (1994) *Proc. Natl. Acad. Sci. USA* **91,** 3014–3018.
10. Predescu, S., Predescu, D. & Palade, G. E. (1997) *Am. J. Physiol* **272,** H937–H949.
11. Predescu, D. & Palade, G. E. (1993) *Am. J. Physiol.* **265,** H725–H733.
12. Griffith, J. Q., Farris, E. J. & Roberts, A. B. E. (1942) in *The Rat in Laboratory Investigation*, eds. Griffith, J. Q., Jr., & Farris, E. J. (Lippincott, Philadelphia), pp. 274–290.
13. Ghitescu, L. & Bendayan, M. (1992) *J. Cell Biol.* **117,** 745–755.
14. Frens, G. (1973) *Nature (London) Phys. Sci.* **241,** 20–22.
15. Roth, J. (1983) in *Techniques in Immunocytochemistry*, eds. Bullok, G. R. & Petrusz, P. (Academic, London), Vol. 2, pp. 216–284.
16. Quagliarello, V. J., Ma, A., Stukenbrok, H. & Palade, G. E. (1991) *J. Exp. Med.* **174,** 657–672.
17. Good, A. H., Wofsy, L., Henry, C. & Kimura, J. (1979) in *Selected Methods in Cellular Immunology*, eds. Mishell, B. B. & Shiigi, S. M. (Freeman, San Francisco), pp. 343–350.
18. Bolton, A. E. & Hunter, W. M. (1973) *Biochem. J.* **133,** 529–539.
19. Morrissey, G. J., Gravelle, D. R., Lo, L. & Powe, J. E. (1992) *Lab. Animal Sci.* **42,** 70–72.
20. Simionescu, N., Simionescu, M. & Palade, G. E. (1972) *J. Cell Biol.* **53,** 365–392.
21. Smith, P. K., Krohn, R. I., Merkmanson, G. T., Mallia, A. K., Gartner, F. H., Provenzano, M. D., Fujimoto, E. K., Goeke, N. M., Olsen, B. J. & Klenk., D. K. (1985) *Anal. Biochem.* **159,** 76–85.
22. McLellan, T. (1982) *Anal. Biochem.* **126,** 94–99.
23. Schnitzer, J. E. & Pinney, E. (1992) *Am. J. Physiol.* **263,** H48–H55.
24. Palade, G. E., Simionescu, M. & Simionescu, N. (1979) *Acta Physiol. Scand. Suppl.* **436,** 11–32.
25. Simionescu, N. (1983) *Physiol Rev.* **63,** 1535–1579.
26. Galis, Z., Ghitescu, L. & Simionescu, M. (1988) *Eur. J. Cell Biol.* **47,** 358–365.
27. Predescu, D., Simionescu, M. & Simionescu, N. (1988) *J. Cell Biol.* **107,** 1729–1733.
28. Schnitzer, J. E., Allard, J. & Oh, P. (1995) *Am. J. Physiol.* **268,** H48–H55.
29. Rothman, J. E. (1994) *Nature (London).* **372,** 54–67.
30. Waters, M. G., Griff, I. C. & Rothman, J. E. (1991) *Curr. Opin. Cell Biol.* **3,** 615–620.
31. Schnitzer, J. E., Liu, J. & Oh, P. (1995) *J. Biol. Chem.* **270,** 14399–14404.
32. Takel, K., McPherson, P. S. & Schmid, S. L. (1995) *Nature (London)* **374,** 186–189.
33. Jones, S. M., Howell, K. E., Henley, J. R., Chao, H. & McNiven, M. A. (1998) *Science* **279,** 573–577.
34. Predescu, S., Predescu, D. & Palade, G. E. (1997) *Mol. Biol. Cell* **8,** 232a (abstr.).
35. Simionescu, M. & Simionescu, N. (1991) *Cell Biol. Rev.* **25,** 1–80.
36. Milici, A. J., Watrous, N. E., Stukenbrok, H. & Palade, G. E. (1987) *J. Cell Biol.* **105,** 2603–2612.
37. Ripe, B. & Haralsson, B. (1994) *Physiol. Rev.* **74,** 163–219.
38. Michel, C. C. (1992) *Annu. Rev. Respir. Dis.* **146,** S32–S36.